Supplementary information

Supplementary Material and Methods

Cell culture

Human embryonic kidney (HEK) 293 cells (Clontech) were cultured in DMEM containing L-Glutamin (Invitrogen) supplemented with 10% FCS (Invitrogen), 0.1 mM nonessential amino acids (Invitrogen) and Penicillin/Streptomycin (Roche). Pooled human microvascular endothelial cells (HMVEC; Lonza), coronary artery smooth muscle cells (CASMC; Lonza), human coronary artery endothelial cells (HCAEC; Lonza) and human cardiomyocytes (HCM; Promocell) were used until the forth passage.

Quantitative real-time RT-PCR (qRT-PCR)

Total RNA was isolated using the RNeasy Plus Mini Kit (Qiagen) according to the manufacturer´s protocol. Afterwards, 1 µg of RNA from each sample was reverse transcribed into cDNA and subjected to quantitative SYBR green PCR (StepOnePlus & Fast SYBR Green Mastermix, Applied Biosystems). GAPDH or RPLP0 expression served as loading control. Primer sequences are available on request.

RT-PCR

Total RNA was isolated from zebrafish embryos using the RNeasy Mini-Kit (Qiagen) following the manufacturer's protocol. First-strand cDNA was generated from normalized RNA amounts using random hexamer primers and the Superscript II kit (Invitrogen). RT-PCR was performed with specific primer pairs: zebrafish actin (413 bp fragment, forward: CTTGCGGTATCCACGAGAC, reverse: GCGCCATACAGAGCAGAA; program: 94°C for 3min (94°C for 45 s, 55°C for 45 s, 72°C for 1 min x 35, 72°C for 10 min), zebrafish HDAC6

XM_688766.2 (253 bp fragment) forward: GTAGACGCCTTCACTCGCTTTC, reverse: AAACCGAGTCATATTTCTCAGCAA; program (95°C for 45 s, 60°C for 45 s, 72°C for 1 min) x 33, 72°C for 10 min), zebrafish cortactin ENSDART00000058468 (137 bp fragment) forward: AAGGAGCAGATGACTGGGAA, reverse: GACCGTCTGACGCAGCTT; program: 95°C for 5 min (95°C for 30 s, 58°C for 30 s, 72°C for 1 min) x 35, 72°C for 5 min.

Flow cytometry

At 24 hpf anesthetized embryos were dechorinated, incubated 15 min in modified Ringer solution (116 mM NaCl, 2.9 mM KCl, 5 mM HEPES, pH 7.2), deyolked, washed in PBS and lysed in 0.25% trypsin for 15-20 min. The reaction was stopped with PBS containing 10% FCS and 2 mM $CaCl_2$, cells were centrifuged and resuspended in buffer (0.5% FCS, 1 mM EDTA in PBS). EGFP-positive cells were sorted using a FACScan flow cytometer running CellQuest software (Becton Dickinson). EGFP-positive and negative cells were then used for RT-PCR.

Microscopy and analysis

For *in vivo* imaging, EGFP-expressing *tg(fli1:EGFP)* embryos were manually dechorionated, anesthetized with 0.003% tricaine and embedded in 1% low-temperature melting agarose (Roth). Fluorescence was analyzed using the confocal microscope DMIRE2 with Leica TCS SP2 True Confocal Scanner (Leica Microsystems). Stacks were recorded as indicated in the overview image. Overview pictures and sections of embryo were analyzed with the fluorescence microscope DMI 6000 B (Leica).

Statistical analysis and quantification

For each morpholino injection the first 17 intersegmental vessels (ISV) from the anterior part of 22-56 embryos (48 hpf) were analysed for impaired ISV. For quantification of the dorsal longitudinal anastomotic vessel (DLAV), DLAV segments between 17 ISVs from the anterior part of 22-56 embryos (48 hpf) were counted. The parachordal vessel (PAV) was quantified in 31-56 embryos (48 hpf) regarding its partial or complete absence. All data were analyzed by Student's *t*-test (2-sided, unpaired). A *P* value of <0.05 was considered as statistically significant.

Whole mount antibody staining

For whole mount antibody stainings *tg(fli1:EGFP)* embryos were fixed 2 h in 4% PFA/PBS, washed, dehydrated in methanol and stored at -20°C. Embryos were rehydrated, permeabilized with proteinase K (Macherey-Nagel) and fixed again with 4% PFA/PBS. After blocking in 1% BSA plus 2% serum in PBST, embryos were incubated with an anti-GFP antibody at 4°C overnight. On the following day embryos were washed for 6 h and the secondary antibody was added at 4°C overnight. The colour reaction was developed using the Vectastain ABC kit with horseradish peroxidase and DAB as a chromogen.

Lysis of zebrafish embryos for Western blot analysis

Embryos were washed, lysed in buffer (150 mmol/L NaCl, 50 mmol/L Tris-HCl, pH 7.4, 1% NP40, 10 mmol/L EDTA, 10% glycerol, and protease inhibitors), followed by homogenization with a syringe.

Virus production

Overexpression virus was produced by co-transfection of HEK 293FT cells with the corresponding lenti-vector (plenti4-V5 DEST), the packaging plasmids pMD2.G and pCMVΔR8.91 (Ziebart et al., 2008) using GeneJuice (Merck) according to the manufacturer´s protocol. Supernatant was harvested 48 h and 72 h after transfection, combined and concentrated using Amicon Ultra-15 filter devices (Millipore).

Transduction of HUVEC

HDAC6 and control shRNA lentiviral particles were purchased from Sigma Aldrich using the following clones: HDAC6: TRCN0000004839 (targeting the 3`UTR of HDAC6); Control: non target control SHC002H. HUVEC cells were seeded 0.5-1.0^5 cells per 6 well plate. For viral transduction of shRNA-virus, 8 µg/ml hexadimethrine bromide (Sigma Aldrich) was added together with the virus, using a multiplicity of transductions of 5 or 10. 48 h after transduction cells were selected with puromycin 0.4 µg/ml till untransduced control cells completely died. Overexpression of HDAC6 and cortactin constructs in HUVEC was achieved by adding of 100 µl 15x concentrated virus supernatant for 24 h.

MTT viability assay

Assessment of cell viability was performed using the MTT [3-(4,5-dimethylthiazol-2-yl)-2,5-diphenyl-2H-tetrazolium bromide] assay. 48 h after transfection, 0.5 mg/ml MTT was added to each well and cells were incubated for 4 h at 37°C. Cells were washed with PBS and lysed 30 min at room temperature with lysis buffer (40 nM HCl in isopropanol). Absorbance was photometrically measured at 550 nm.

Transwell migration and scratched wound assay

Transwell migration was performed as described previously (Carmona et al., 2009).

Transwell membranes were coated on both sides with fibronectin (2.5 µg/ml; Roche) for 1 h at room temperature. Cells were allowed to migrate for 4 h towards the lower chamber. Scratched wound assay was performed as described previously (Diehl et al., 2007).

Western blot analysis

For Western blot analysis, cells were lysed in RIPA lysis buffer (Sigma) for 15 minutes on ice. After centrifugation for 15 minutes at 20.000 x g (4°C), the protein content of the samples was determined according to the Bradford method. Equal amounts of protein were loaded onto SDS-polyacrylamide gels and blotted onto PVDF membrane. Western blots were performed by using antibodies directed against HDAC6 (Santa Cruz clone H-300 and Millipore clone CT), cortactin (Millipore clone 4F11), acetyl-tubulin (Sigma Aldrich clone 6-11B-1), α-tubulin (NeoMarkers clone DM1A and RB9281), V5 (Sigma Aldrich clone V5-10), Flag (Sigma Aldrich clone M2), acetyl-lysine (Immunechem), pan-actin (Dianova clone Ab-5). Secondary antibodies were purchased from Jackson ImmunoResearch. Densitometry was performed where indicated for the quantification of the Western blots using the Scion Image software (version 4.0.2, Scion, Frederick, MD).

Immunoprecipitation

Cells were washed one time with PBS and lysed with lysis buffer containing 50 mM Tris (pH 7.5), 120 mM NaCl, 0.5 mM EDTA, 0.5% Nonidet P-40 and protease inhibitor cocktail (Roche) on ice for 30min. After centrifugation for 15 min at 20.000 x g (4°C), the protein content of the samples was determined according to the Bradford method. Equal amounts of protein were pre-incubated with 20 µl A/G agarose beads (Santa Cruz) for 1 h at 4°C under agitation. Protein lysates were incubated with the indicated antibody or with Flag-antibody-coupled beads (Sigma Aldrich) at 4°C overnight under agitation. As control IP serves mouse

IgG (mouse IgG1 isotype control (RD system) or mouse IgG1 κ isotype control (BD Pharmingen)) or rabbit IgG (negative control rabbit immunoglobulin fraction (Dako)). Antibody complexes were collected by incubation with A/G agarose beads for 2 h. Beads were washed 3 times with lysis buffer and boiled with loading buffer for Western blot analysis.

For determination of the acetylation level of cortactin, HUVEC were transduced with myc-tagged cortactin wt virus. After treatment, cells were lysed in RIPA buffer containing protease inhibitor cocktail (Roche). To inhibit the activity of HDACs during the lysis and the immunoprecipitation broad spectrum HDAC inhibitors TSA 1 µg/ml (class I and II) and nicotinamide 20 mM (class III) were added. Immunoprecipitation was performed as described above using anti-acetyl-lysine beads (Immunechem).

Immunofluorescence staining

Cells were seeded 24 h prior staining on 8 chamber microscope slides coated with 2.5 µg/ml fibronectin for 1 h at room temperature. For immunofluorescence staining, HUVEC were washed with PBS, fixed with 4% paraformaldehyde and permeabilized with 0.02% saponin (Sigma Aldrich). Unspecific binding was blocked with 3% BSA for 1 h at room temperature. Cells were incubated with indicated primary antibodies overnight at 4°C in 3% BSA. After washing, Alexa 488- or Alexa 594-conjugated secondary antibody was added for 1h at room temperature with or without FITC- or TRIC-labeled phalloidine. Nuclei were stained using Hoechst 33342 and cells were embedded in mounting media. Pictures were taken with an Axio Observer Z1 (Axio Vision Rel 4.8, Carl Zeiss, Jena) using the Plan-Apo 63x 1.4 oil DIC II objective.

α-tubulin and acetyl-α-tubulin ELISA

For measuring total α-tubulin the pathscan total α-tubulin sandwich ELISA kit (Cell Signaling Technology) was used according to the manufacturer instruction. Acetyl-α-tubulin was measured using the pathscan total α-tubulin sandwich ELISA kit (Cell Signaling Technology) by substitution of the first detection antibody with the acetyl-tubulin antibody (Sigma Aldrich clone 6-11B-1) 1:1000 in wash buffer. To block endogenous HDAC activity 1 μM TSA was added to the lysate.

Shear stress

HUVEC were exposed to laminar shear stress (20 dyn/cm^2) for 72 h using in flow channels (μ-Slide I 0.4 Luer combined with the ibidi pump system, ibidi, Martinsried, Germany).

Retina model

Eyes of HDAC6 $^{-/-}$ or HDAC6 $^{+/+}$ littermates at day P5 were removed and the eyes were fixed for 2h with 4% formaldehyde on ice. After 3 times washing, the retina was dissected and the hyaloid vessels were removed. The retinas were washed with PBlec buffer for 20 min and incubated in direct conjugated isolectin-B4 (Invitrogen #I21411 500 μg / 500 μl PBlec) 1:100 in PBlec overnight at 4°C. Retinas were washed in PBS, post-fixed in 4% formaldehyde for 5 min and mounted for microscopic analysis. Pictures were taken using laser scanning microscope (LSM510 META with Software Release 4.0 SP2, Carl Zeiss, Jena).

Tumor model

Lewis lung carcinoma cells (LLC1, ATCC CRL-1642) were cultured in DMEM containing Glutamax™ and sodium pyruvate (Invitrogen) supplemented with 10% FCS and Penicillin/Streptomycin (P/S, Roche). 1 million LLC1 cells were injected subcutaneously in 3 to 4 month old HDAC6$^{+/+}$ or HDAC6$^{-/-}$ mice. Tumor volume was measured at the indicated

time points with a Thorpe caliper (Horex, Germany) and was calculated as L1 x L2. After explantation, tumors were weighted and 3D tumor volume was calculated using the formula: volume = $[1/2*(L*W^2)]$, where L is length of the tumor and W is width of tumor. Tumor specimens were fixed in 4% formalin and were histologically examined. Sections were stained with an anti-endomucin antibody (eBioscience; 1:100) followed by an anti-rat Alexa Fluor 488 antibody (Invitrogen). Pictures were taken with a laser scanning microscope (LSM510 META with Software Release 4.0 SP2, Carl Zeiss, Jena) using the Plan-Neofluar 40x/1.3 Oil objective. 5 images per tumor were evaluated manually.

Supplementary figure legend:

Supplementary figure 1: HDAC6 expression and effect of HDAC6 silencing on endothelial sprouting, tube formation and migration. A/B) HCM: human cardiomyocytes; HCASMC: human coronary artery smooth muscle cells; HMVEC: human microvascular endothelial cells; HUVEC: human umbilical vein endothelial cells; HCAEC: human coronary artery endothelial cells. A) Relative HDAC6 mRNA expression in different endothelial and non-endothelial cells. Expression data were normalized to GAPDH expression (n=3-4). B) Western Blot analysis of HDAC6 expression in different endothelial and non-endothelial cells. α-tubulin expression was used as loading control. C) Relative mRNA expression of HDAC6 and HDAC9 24 h after transfection with three independent HDAC6 or two control siRNAs in HUVEC. Data were normalized to GAPDH expression. Data are presented as % of the mean of the two control siRNAs (n=3). D) Effect of HDAC6 silencing on HUVEC viability measured by MTT assay 24 h and 48 h after transfection with siRNA. Results are shown as % of the mean of two control siRNAs (n=3). E/F) HUVEC were transfected with either control siRNA or three different HDAC6 siRNAs for 24 h and subjected to a spheroid assay (n=5). E) Quantification of the number of sprouts per spheroid. F) Quantification of the number of branch points per spheroid. G) Quantification of capillary-like tube formation of HUVEC on matrigel after HDAC6 silencing. HUVEC were transfected with either two different HDAC6 or two different control siRNAs for 24 h and seeded on matrigel for 24 h. Cumulative tube length was measured. As control serve the mean of the two control siRNAs (n=4). Representative images are shown in the lower panel. H) Quantification of HUVEC scratched wound migration 24 h after siRNA transfection with either HDAC6 siRNA or control siRNA. The following siRNAs were used: siHDAC6 III and siScr: 5`-AGCGUGUAGCUAGCAGAGG-`3 (n=3).

Supplementary figure 2: Silencing of HDAC6 does not affect the position of HDAC6 depleted cells within the growing sprouts. A/B) *In vitro* cell fate assay. HUVEC were either labeled with YFP or CFP fluorescent protein by transduction with virus encoding for YFP or CFP. The CFP expressing cells were transfected with control siRNA whereas the YFP expressing cells were transfected with HDAC6 siRNA. Both populations were mixed and spheroids were generated. Sprouting was stimulated with 20 ng/ml FGF2. After 24 h, cells were fixed and nuclei were stained with DAPI. Confocal images were taken with a laser scanning microscope using a Plan-Neofluar 20x/0.5 objective. A) Quantification of total sprouted cells, number of tip cells and number of stalk cells per color and spheroid (n=3). B) Representative image showing nuclei in blue, HDAC6 siRNA transfected cells in red and control siRNA transfected cells in green. **Hypoxia up-regulates HDAC6 expression.** C) HUVEC were exposed to static or shear stress conditions for 72 h. Relative HDAC6 mRNA expression was normalized to RPLP0 expression (n=3). D/E) HUVEC were grown under normoxic or hypoxic conditions (1% O_2, 5%CO_2) for 24 h. Relative mRNA expression was normalized to RPLP0 expression (n=6). D) Relative HDAC6 mRNA expression. E) Relative VEGF mRNA expression was measured as positive control for hypoxic conditions. F) HUVEC were grown for 36 h under normoxic or hypoxic conditions (1% O_2, 5% CO_2). HDAC6 protein expression was analyzed by Western blot. α-tubulin expression was used as loading control (n=5). G) Densitometric quantification of F.

Supplementary figure 3: HDAC6 is expressed in the vessels of zebrafish embryos. A) Flow cytometric separation of GFP-positive cells from *tg(fli1:EGFP)* zebrafish line. EGFP-positive cells were sorted using a FACScan flow cytometer running CellQuest software. Lower table shows the purity of the sorted cell populations. B) Expression of HDAC6 was analyzed by RT-PCR yielding a band at 253 bp. An unspecific band was detected at 700-800 bp. For equal loading serves actin expression (see Supplementary figure 7A). C) Design of

HDAC6 morpholinos for silencing of HDAC6 expression during zebrafish embryonic development. Translation-blocking morpholino (TB-Mo) targets the start codon of *Danio rerio* HDAC6 mRNA and inhibits translation of mRNA. The splice-blocking morpholino (SB-Mo) targets the exon-5-intron-5 boundary. The scheme indicates the possible splice products and the calculated PCR product sizes. HDAC6 SB-Mo leads to a non-splicing of intron 5 thereby introducing a frameshift of the mRNA. Exons are shown in blue and introns are shown in green. Numbers indicate number of exon or intron. PCR primer positions are indicated. Mo: morpholino; ATG: start codon; E: exon; I: intron. **Specificity of shHDAC6 virus and experimental setup for in vivo spheroid assay in mice.** D) HUVEC were transduced with control or HDAC6 shRNA virus for long-time silencing of HDAC6. After 7 days, HUVEC were lysed and HDAC6 and acetyl-tubulin levels were analyzed by Western blot. α-tubulin serves as loading control. E) HUVEC were stably transduced with either shControl or shHDAC6 virus for long-time silencing of HDAC6. In a second step of transduction, shControl and shHDAC6 cells were transduced either with GFP or HDAC6 wt virus for 24 h and subjected to a spheroid assay (n=4). F) Scheme of the *in vivo* spheroid assay in mice. **HDAC6 knockout mice do not show a reduced retinal vessel outgrowth.** G/H) Eyes of HDAC6$^{-/-}$ or HDAC6$^{+/+}$ littermates at day P5 were removed and the retina was prepared. Vessels were stained by isolectin B4. G) Representative images of retinas. H) Quantification of retinal outgrowth (n= 4 for HDAC6$^{+/+}$; n=18 for HDAC6$^{-/-}$).

Supplementary Figure 4: HDAC6 knockout mice show an increased tumor growth whereas tumor vascularization is unaffected. LLC1 tumor cells were subcutaneously injected in male mice (A-D) and female mice (E-I). A and E) Tumor size was measured at the indicated time points. d=days B/C and F/G) Tumor volume and tumor weight were detected in explanted tumors at day 19 (A-C: n=4 for HDAC6$^{+/+}$ and n=6 for HDAC6$^{-/-}$; E/F: n=6 for

HDAC6$^{+/+}$ and n=8 for HDAC6$^{-/-}$) D and H) Tumor angiogenesis was detected in sections stained with the endothelial marker endomucin. A secondary antibody conjugated to Alexa Fluor 488 was used. The number of vessels was counted manually (n=4 for HDAC6$^{+/+}$ and n=4 for HDAC6$^{-/-}$). I) Representative images of endomucin stained tumor vessels (green) in female mice. Nuclei are shown in blue. J) mRNA Expression of HDAC6 in cultured HUVEC and human CD3^{+} and CD14^{+} cells isolated from blood. RNA was isolated, reverse transcribed and used for real-time PCR. Expression was normalized to total RNA (n=3-4).

Supplementary figure 5: HDAC6 facilitates angiogenesis dependent on its deacetylation activity but independent of α-tubulin deacetylation. A) HUVEC were treated with DMSO (control), the HDAC6-specific inhibitor tubacin or the non-active derivative niltubacin for 24 h. Protein lysates were subjected to Western blot analysis with HDAC6-, actetyl-tubulin- and α-tubulin specific antibodies. α-tubulin serves as loading control. B) HUVEC were treated with 10 μM tubacin for 24 h and ratio of acetylated α-tubulin to total α-tubulin was determined by ELISA. Data are presented in arbitrary units (n=3). C) Spheroid assay (upper panel), scratched wound migration assay (lower left panel) and tube formation assay (lower right panel) were performed with untreated HUVEC. HDAC6-specific inhibitor tubacin or the non-active derivative niltubacin were added after start of the assay in HUVEC medium for 24 h. DMSO alone serves as control (n=3 for spheroid assay, n=4 for scratched wound assay; n=4 for tube formation assay). D) Summary and description of the controversial literature describing the deacetylation activity of single point mutations in either one or both deacetylation domains of HDAC6. Deacetylation activity is divided in global deacetylation activity (upper table), which is usually measured by deacetylation of histone proteins in cell free assays, and α-tubulin deacetylation activity (lower table), which is usually measured *in vitro*. The group of Stuart Schreiber showed that single mutation in either of the domains does

not affect global deacetylation activity assessed by histone deacetylation (Grozinger et al., 1999; Haggarty et al., 2003), while a mutation in the second deacetylation domain inhibits α-tubulin deacetylation (Haggarty et al., 2003). In contrast, the group of Patrick Matthias shows that single mutations in either of the two deacetylation domains inhibits α-tubulin and histone deacetylation (Zhang et al., 2003). A third independent study demonstrates that only the second deacetylase domain exhibits catalytic activity towards α-tubulin as well as histones (Zou et al., 2006). References are indicated. E) HUVEC overexpressing different HDAC6 constructs were treated for 4 h with 2.5 μM tubacin following washout of the inhibitor. Cell lysates were taken 90 min after washout and levels of acetylated α-tubulin and total tubulin were measured by Western blot. Total α-tubulin serves as loading control. F) HUVEC were stably transduced with HDAC6 wt and deacetylation-deficient HDAC6 (HDAC6 H216/611A) virus for 72 h followed by a transwell migration assay under basal condition. As control serves mock transduced cells. Data are shown as % mock control.

Supplementary figure 6: HDAC6 and cortactin co-localize with actin at the cell membrane. A) HUVEC were stained for cortactin with a cortactin-specific antibody (Alexa 594-conjugated secondary antibody; shown in red) and FITC-phalloidin (shown in green) for actin fibers. Nuclei were stained with Hoechst 33342 (shown in blue). White arrow indicate co-localization of cortactin with actin fibers. B) HUVEC were stained for HDAC6 with a HDAC6-specific antibody (Alexa 488-conjugated secondary antibody; shown in green) and TRIC-phalloidin (shown in red) for actin fibers. Nuclei were stained with Hoechst 33342 (shown in blue). White arrows indicate co-localization of HDAC6 with actin fibers. The lower panel shows a higher magnification of the staining at the leading edge of a HUVEC. **HDAC6 interacts with cortactin in endothelial cells and silencing of HDAC6 increases acetylation of cortactin in HUVEC.** C) HUVEC were transiently transfected with Myc-tagged cortactin wt plasmid for 24 h. Immunoprecipitation of protein lysates was performed

using a HDAC6-specific antibody or control IgG antibody. The ability of cortactin to bind HDAC6 was assessed by Western blot of the precipitate using a cortactin-specific antibody (lower panel). HDAC6 expression and cortactin overexpression was analyzed by Western blot of total cell lysates. GFP-transduced HUVEC serve as control for overexpression (upper panel) (n=2). D) HUVEC were transiently transfected with Flag-tagged HDAC6 wt plasmid for 24 h. Immunoprecipitation of protein lysates was performed using a cortactin-specific antibody or control IgG antibody. The ability of HDAC6 to bind cortactin was assessed by Western blot of the precipitate using a HDAC6-specific antibody (lower panel). Cortactin expression and HDAC6 overexpression was analyzed by Western blot of total cell lysates. GFP-transduced HUVEC serve as control for overexpression (upper panel) (n=3). E) HUVEC were stably transduced with V5-tagged cortactin wt virus and subsequently transfected with HDAC6 or control siRNA for 72 h. Equal amounts of protein lysates were subjected to immunoprecipitation reaction with anti-V5 antibody agarose beads. Bound proteins were resolved and used for Western blot analysis of cortactin acetylation levels utilizing anti-acetyl-lysine specific antibody. V5-cortactin immunoprecipitates serve as equal loading. HDAC6, cortactin and α-tubulin levels were measured in total cell lysates.

Supplementary figure 7: Cortactin is crucial for vessel formation in zebrafish embryos. A) GFP-positive and GFP-negative cells from 24 h old *tg(fli1:EGFP)* zebrafish were subjected to RT-PCR to analyze the expression of cortactin and actin. PCR yields a band at 137 bp for cortactin and 413 bp for actin. PCR without template serves as negative control. B) Aberrant splicing of *Danio rerio* cortactin mRNA after cortactin splice-blocking morpholino (SB-Cortactin-Mo) injection into zebrafish embryos (24 h post fertilization). Left panel: Morpholino injection leads to splicing of exon 2 yielding a signal at 63 bp compared to wild-type (137 bp). The origin of the additional signals in the SB-cortactin-Mo condition is currently unknown. Schematic presentation of morpholino function is shown in the right

panel. For further explanation see Suppl. Fig. 3C. C-F) Phenotyping of cortactin morphants and control morphants 48 h post fertilization (n=31-33) C) Parachordal vessel phenotype in cortactin morphants. Parachordal vessel phenotype was classified as absent, partial absent or present. Data shows percentage of animals with indicated phenotype. Control morpholino serve as control. D) Quantification of parachordal vessel phenotype from C) with absent = 0, partial absent = 1 and present = 2. E) Quantification of ISV defects per animal. F) Quantification of DLAV defects per animal. G) Quantification of ISV and DLAV diameter in cortactin morphants. 48 h post fertilization the diameter of 5 ISVs and 5 connecting DLAVs was measured at the yolk sac extension of control and cortactin morphants (n=31).

Supplementary figure 8: Deacetylation mimic cortactin rescues the defective migration after HDAC6 depletion A) HUVEC were stably transduced with HDAC6 or control shRNA virus, and subsequently transduced with mock control or different cortactin constructs (for explanation of cortactin constructs see figure legend 6E) as indicated. Western blot analysis of HDAC6 silencing and cortactin overexpression (n=3). B) HUVEC were stably transduced with HDAC6 or control shRNA virus, and subsequently transduced with mock control or different cortactin constructs (for explanation of cortactin constructs see figure legend 6E) as indicated. Quantification of migration in a transwell migration assay under basal conditions. Data are presented as % shControl + Mock (n=3). **Deacetylation mimic cortactin rescues vessel defects after HDAC6 depletion in zebrafish embryos.** C) Cortactin 9KR was subcloned in pCS2plus using BamHI and EcoRI. For *in vitro* transcription, the vector was NotI-linearized and sense mRNA was transcribed using SP6 promotor. Quality of mRNA was controlled on a denaturating RNA gel with a main band at approximately 2200 bp. D) Quantification of parachordal vessel defects in ATG-HDAC6-morphants with or without 100 pg of cortactin 9KR-mRNA 48 h post fertilization. As control group serves 100 pg of cortactin 9KR-mRNA. Quantification of phenotype with absent = 0, partial absent = 1 and

present = 2 (n=56 for ATG-HDAC6-Mo; n=49 for ATG-HDAC6-Mo + cortactin 9KR-mRNA; n=48 for cortactin 9KR-mRNA). E) Representative images of D. Arrows indicate vessel defects.

Supplementary Figure 9: Silencing of HDAC10 in HUVEC does not affect endothelial sprouting and the acetylation of cortactin but overexpression of HDAC10 rescues vessel defects caused by HDAC6 depletion in zebrafish. A) Relative mRNA expression of HDAC10 24 h after transfection with siHDAC10 or control siRNA in HUVEC. Data were normalized to RPLP0 expression (n=4). siHDAC10: 5`-GCCUUUCCUGCGAGAGUCA-3`. B) Capillary-like sprouting from HUVEC spheroids was measured after HDAC10 silencing. The spheroid assay was performed 24 h after siRNA transfection. Data are shown as cumulative sprout length per spheroid (n=3). C) HUVEC were stably transduced with V5-tagged cortactin wt virus followed by HDAC10 or control siRNA transfection for 72 h. Equal amounts of protein lysate were subjected to immunoprecipitation reaction with anti-acetyl-lysine antibody conjugated to agarose beads. Bound proteins were resolved and used for Western blot analysis of cortactin acetylation levels utilizing anti-cortactin-specific antibody. HDAC10 and acetylated α-tubulin levels were measured in total cell lysates. As loading controls serve α-tubulin, HDAC6 and cortactin-V5 expression in total cell lysates before precipitation (n=3). D) *Danio rerio* HDAC10 cDNA clone in pME18S-FL was obtained from Imagene (clone BC044446 corresponding NM_199775.1) and subcloned in pCS2plus using EcoRI and XbaI. For *in vitro* transcription, the vector was KpnI-linearized and sense mRNA was transcribed using SP6 promotor. Quality of mRNA was controlled on a denaturating RNA gel with a main band at approximately 2800 bp. E/F) Quantification of vessel defects in ATG-HDAC6-morphants with or without 100 pg of *Danio rerio* HDAC10 mRNA 48 h post fertilization. As control group serves 100 pg of HDAC10 mRNA (n=69 for ATG-HDAC6-Mo; n=55 for ATG-HDAC6-Mo + HDAC10 mRNA; n=52 for HDAC10 mRNA). E)

Quantification of ISV and DLAV defects. Data are presented as % of ATG-HDAC6-Mo. *p<0.05 for ISV; #p<0.05 for DLAV. F) Quantification of parachordal vessel phenotype with absent = 0, partial absent = 1 and present = 2. G) Representative images of E and F. Arrows indicate vessel defects.

References:

Carmona G, Gottig S, Orlandi A, Scheele J, Bauerle T, Jugold M, Kiessling F, Henschler R, Zeiher AM, Dimmeler S, Chavakis E (2009) Role of the small GTPase Rap1 for integrin activity regulation in endothelial cells and angiogenesis. *Blood* **113:** 488-497

Diehl F, Rossig L, Zeiher AM, Dimmeler S, Urbich C (2007) The histone methyltransferase MLL is an upstream regulator of endothelial-cell sprout formation. *Blood* **109:** 1472-1478

Grozinger CM, Hassig CA, Schreiber SL (1999) Three proteins define a class of human histone deacetylases related to yeast Hda1p. *Proc Natl Acad Sci U S A* **96:** 4868-4873

Haggarty SJ, Koeller KM, Wong JC, Grozinger CM, Schreiber SL (2003) Domain-selective small-molecule inhibitor of histone deacetylase 6 (HDAC6)-mediated tubulin deacetylation. *Proc Natl Acad Sci U S A* **100:** 4389-4394

Zhang Y, Li N, Caron C, Matthias G, Hess D, Khochbin S, Matthias P (2003) HDAC-6 interacts with and deacetylates tubulin and microtubules in vivo. *EMBO J* **22:** 1168-1179

Ziebart T, Yoon CH, Trepels T, Wietelmann A, Braun T, Kiessling F, Stein S, Grez M, Ihling C, Muhly-Reinholz M, Carmona G, Urbich C, Zeiher AM, Dimmeler S (2008) Sustained persistence of transplanted proangiogenic cells contributes to neovascularization and cardiac function after ischemia. *Circ Res* **103:** 1327-1334

Zou H, Wu Y, Navre M, Sang BC (2006) Characterization of the two catalytic domains in histone deacetylase 6. *Biochem Biophys Res Commun* **341:** 45-50

Supplementary Figure 1: Kaluza et al.

EMBOJ-2011-77252R

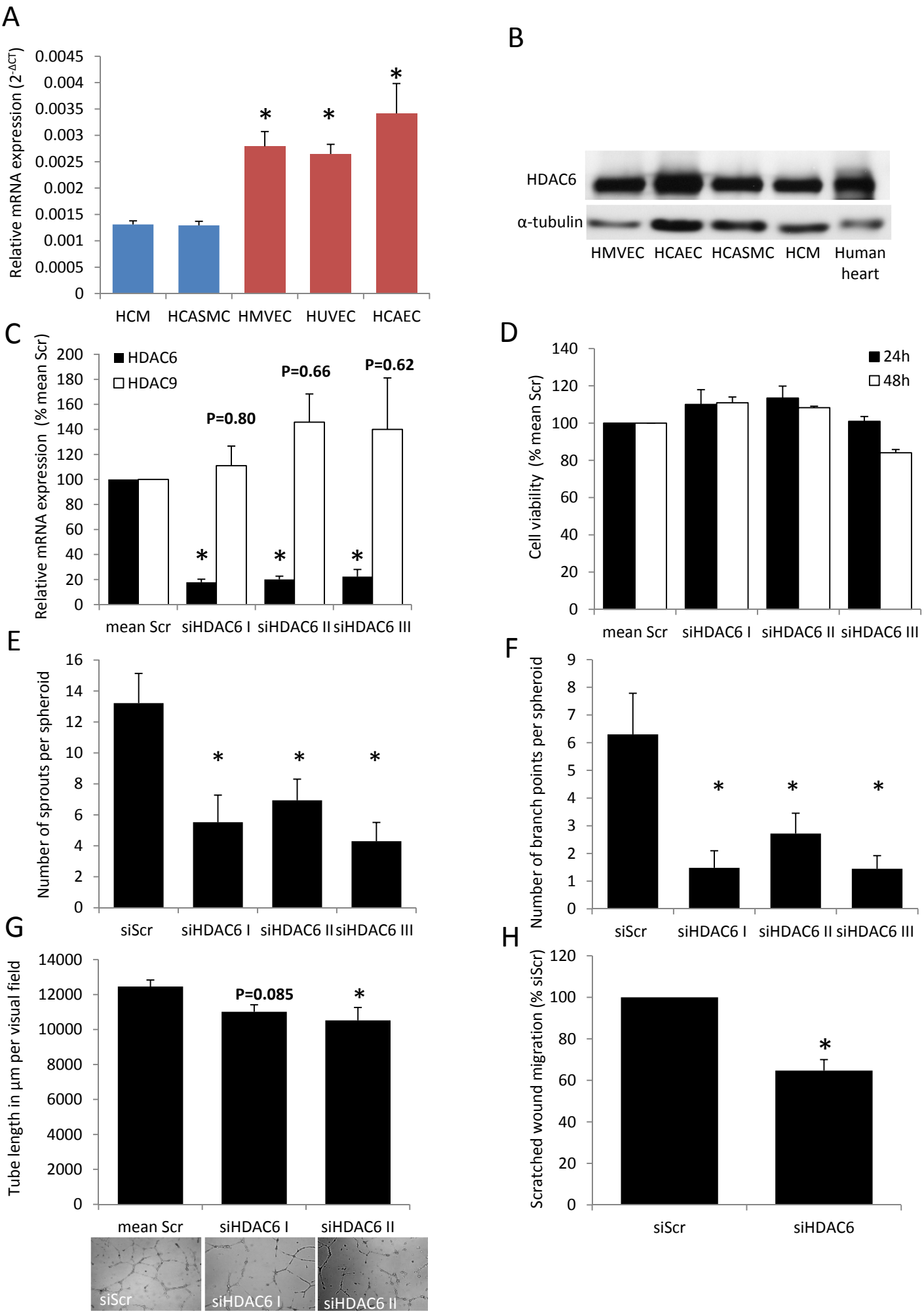

Supplementary Figure 2: Kaluza et al.

EMBOJ-2011-77252R

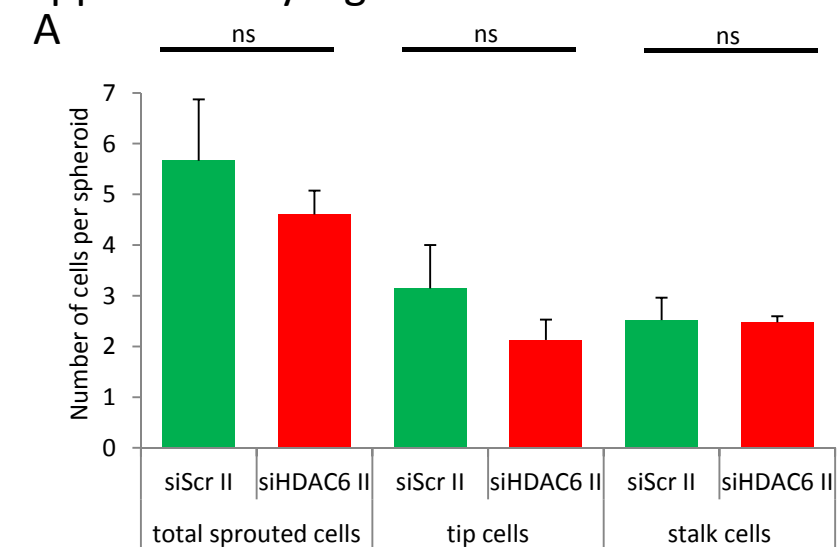

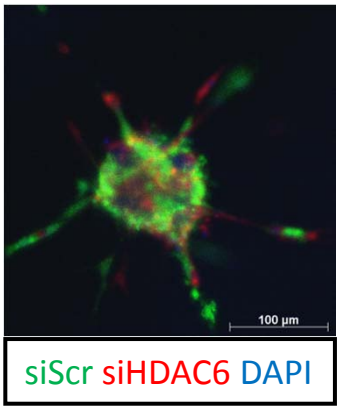

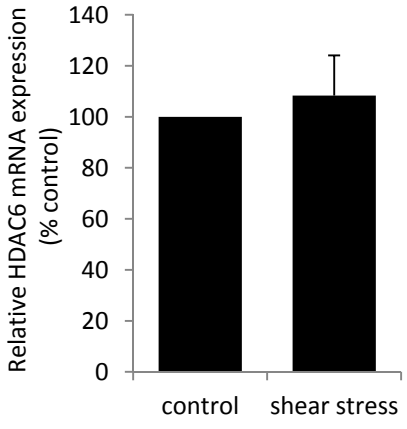

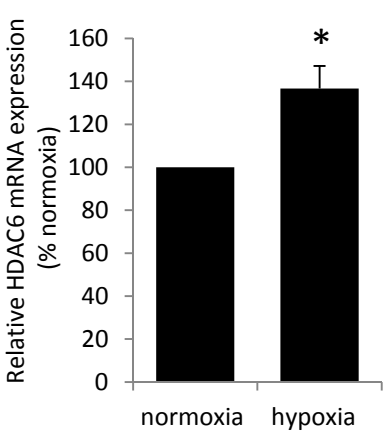

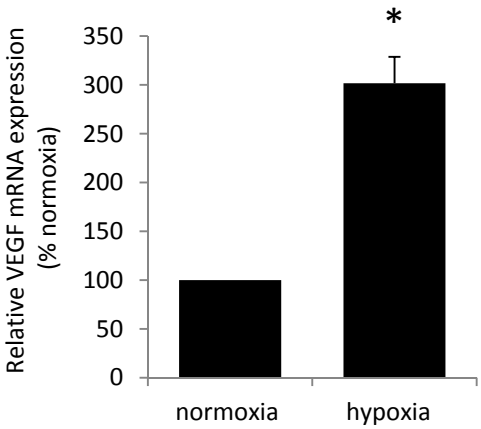

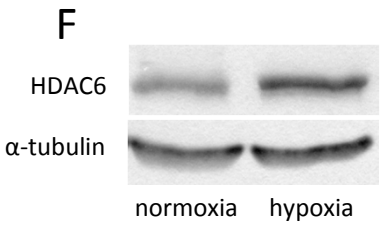

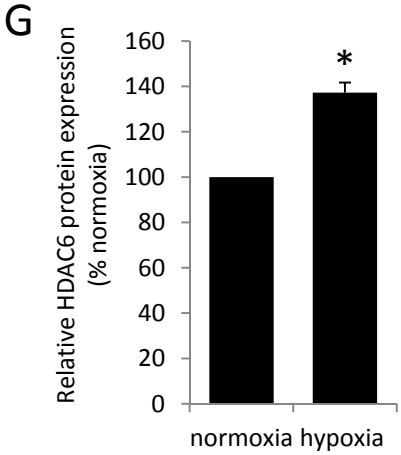

Supplementary Figure 3: Kaluza et al.

EMBOJ-2011-77252R

A

	Purity GFP+	Purity GFP-
Post sort Fli:GFP+	99.1%	0.9%
Post sort Fli:GFP-	0.0%	99.9%

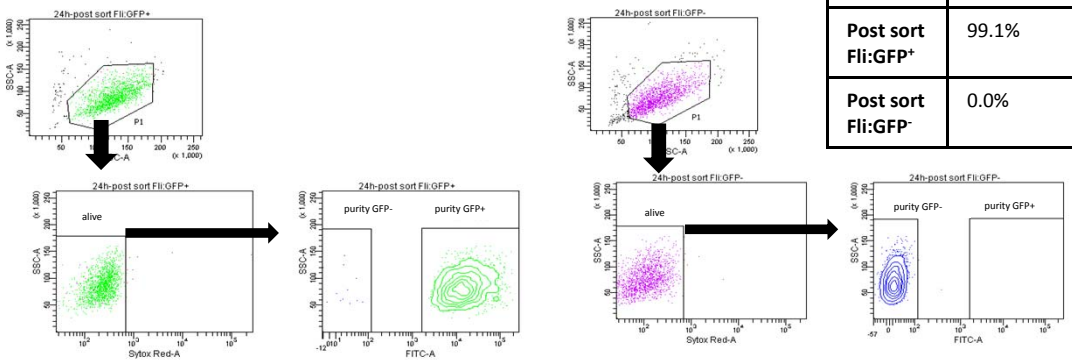

B

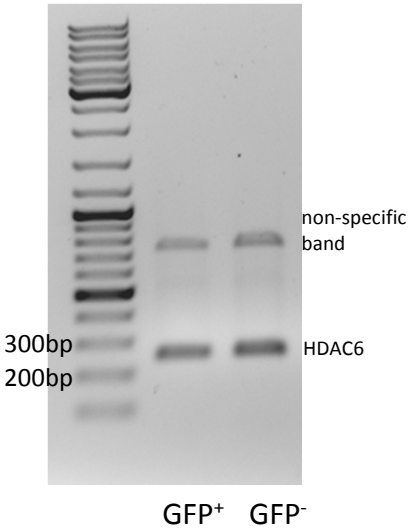

C

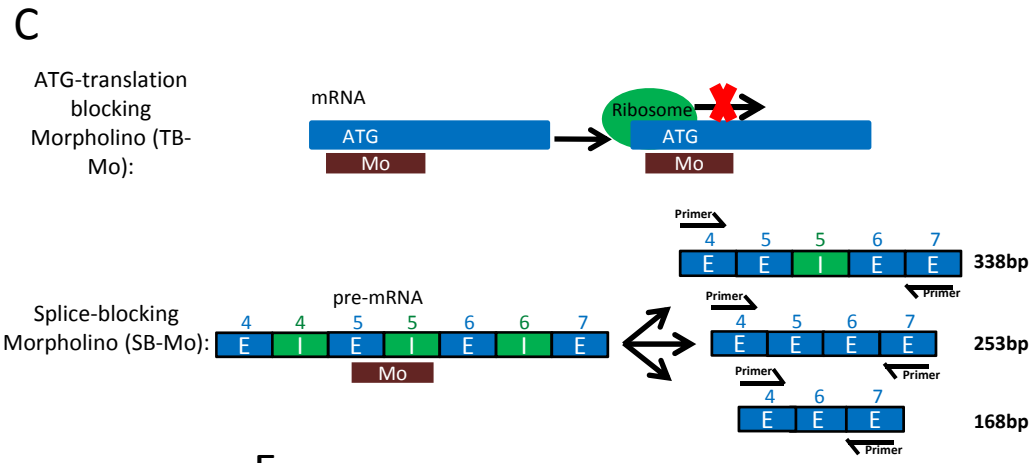

D

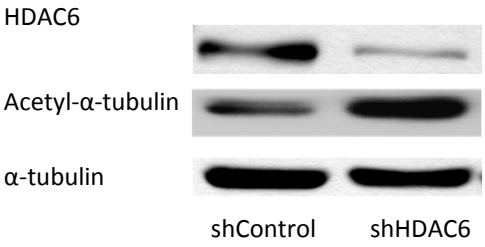

E

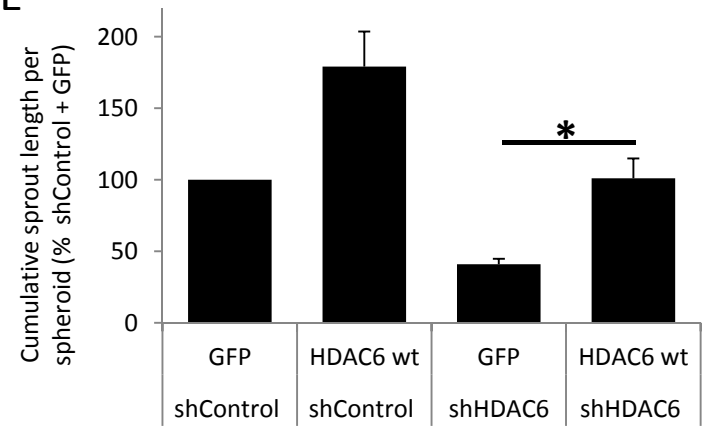

F

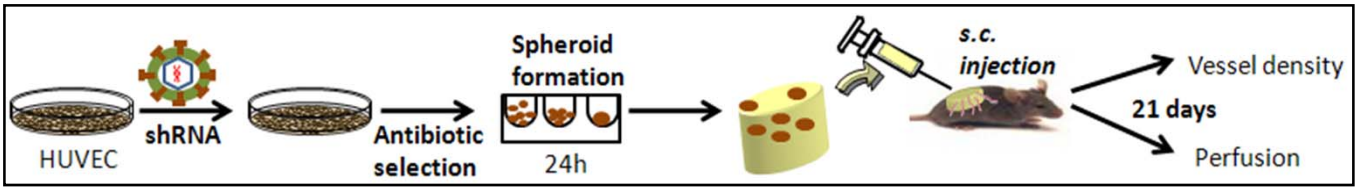

G

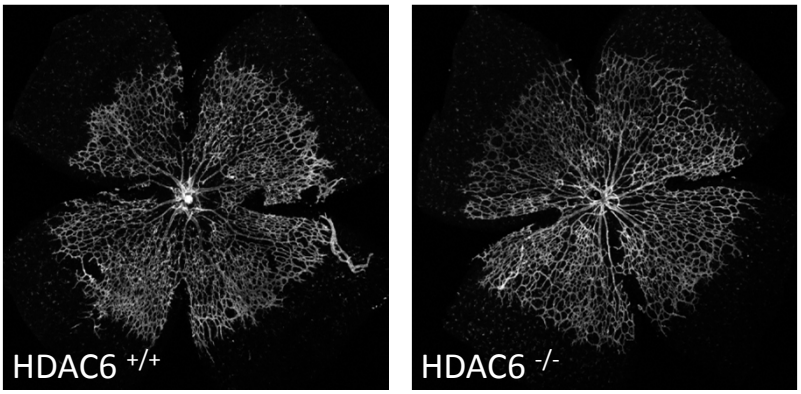

H

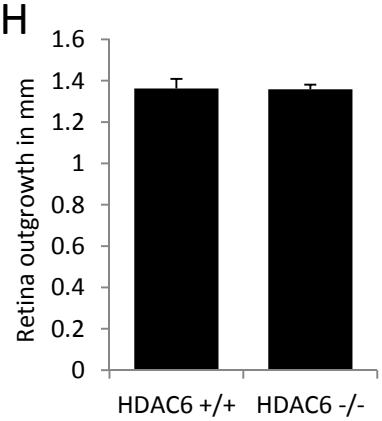

Supplementary Figure 4: Kaluza et al.

EMBOJ-2011-77252R

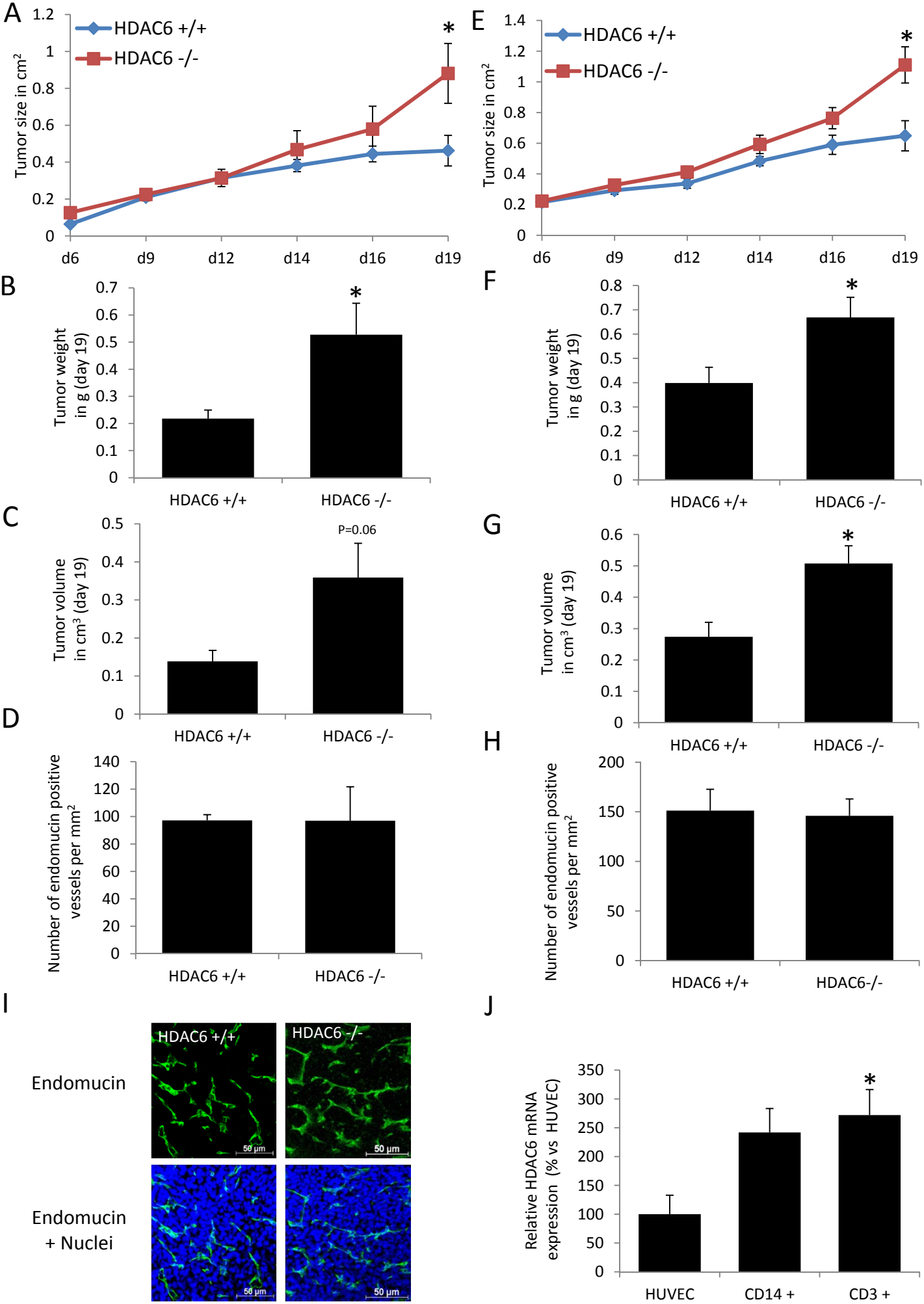

Supplementary Figure 5: Kaluza et al.

EMBOJ-2011-77252R

A

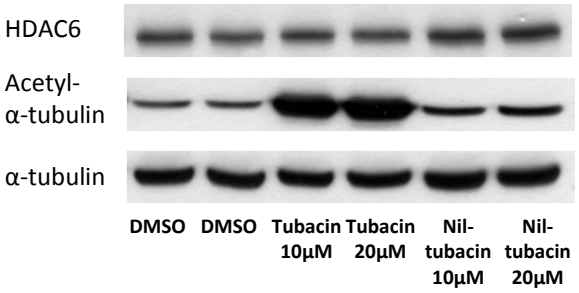

B

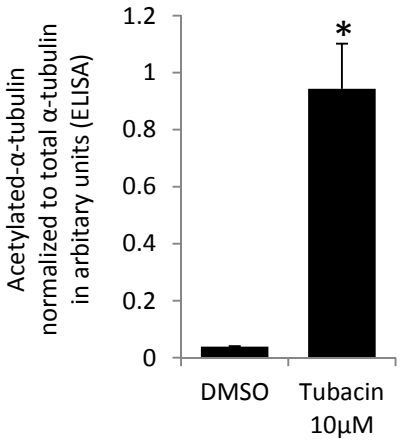

C

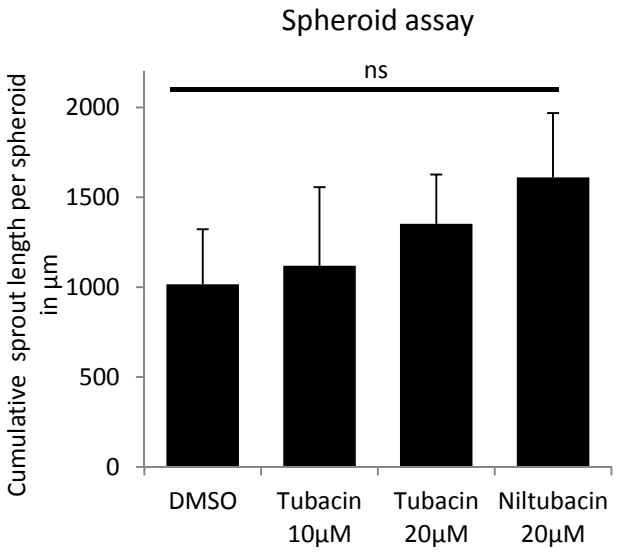

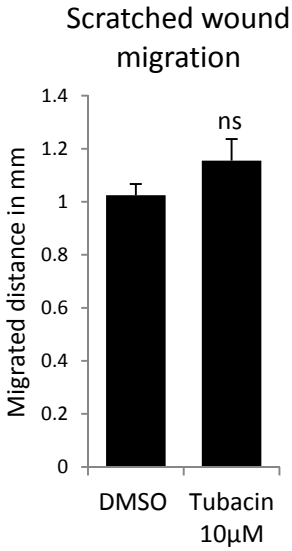

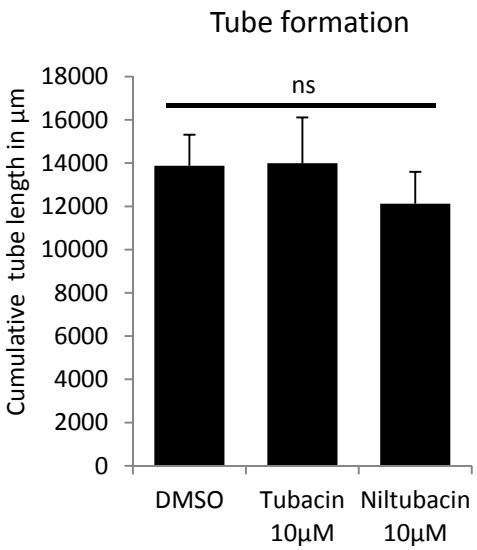

D

Global/ histone deacetylase activity	Grozinger et al. PNAS 1999 and Haggarty et al. PNAS 2003	Zhang et al. EMBO 2003	Zou et al. BBRC 2006
HDAC6 wt	+	+	+
HDAC6 H216A	+	-	+
HDAC6 H611A	+	-	-
HDAC6 H216/611A	-	-	-

α-tubulin deacetylase activity	Grozinger et al. PNAS 1999 and Haggarty et al. PNAS 2003	Zhang et al. EMBO 2003	Zou et al. BBRC 2006
HDAC6 wt	+	+	+
HDAC6 H216A	+	-	+
HDAC6 H611A	-	-	-
HDAC6 H216/611A	-	-	-

E

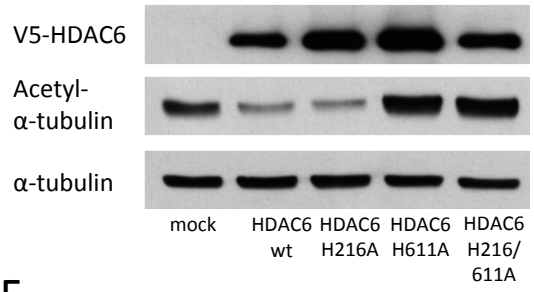

F

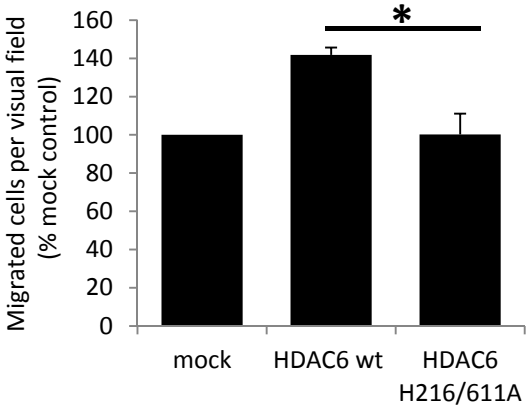

Supplementary Figure 6: Kaluza et al.

EMBOJ-2011-77252R

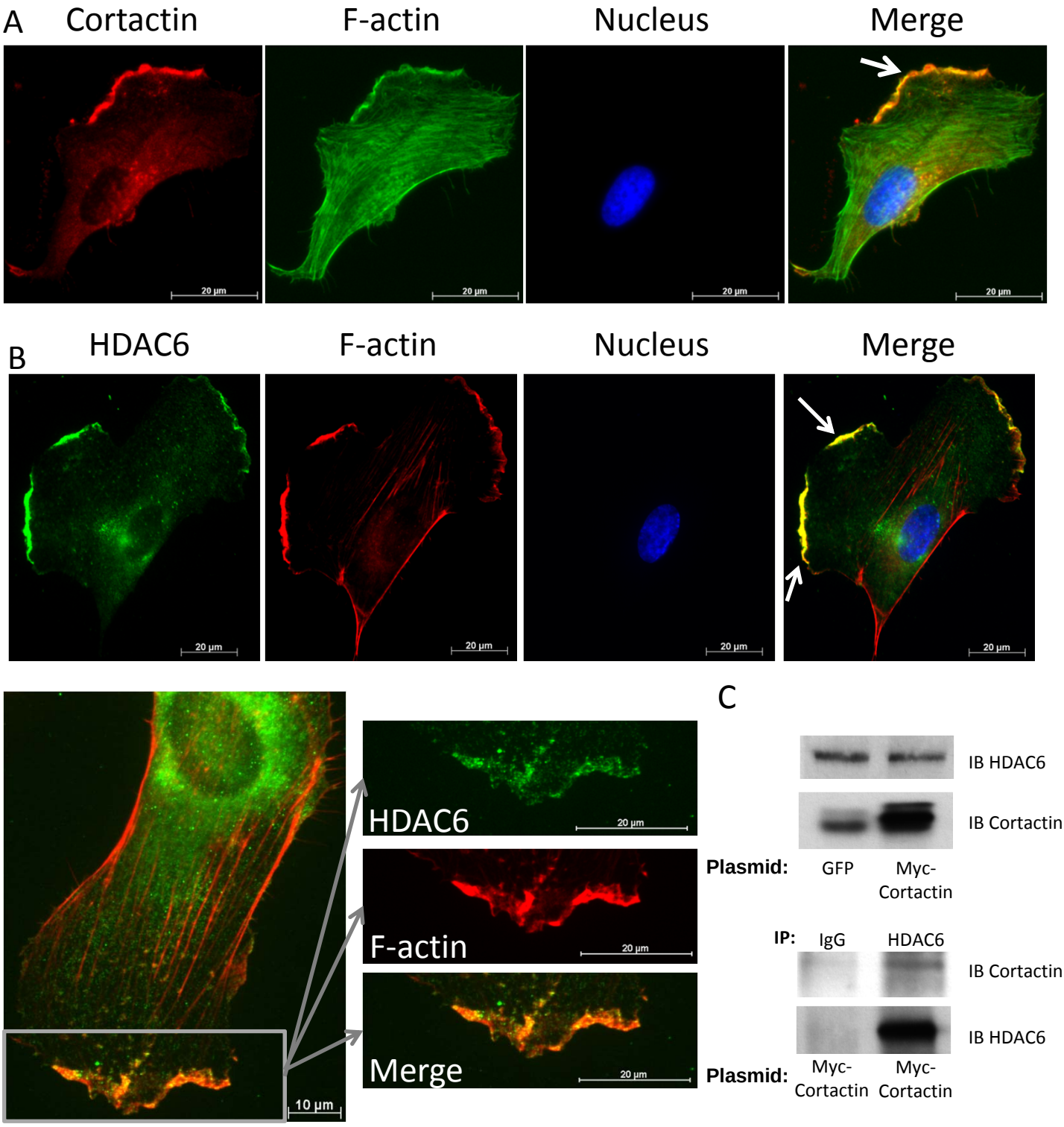

Supplementary Figure 7: Kaluza et al.

EMBOJ-2011-77252R

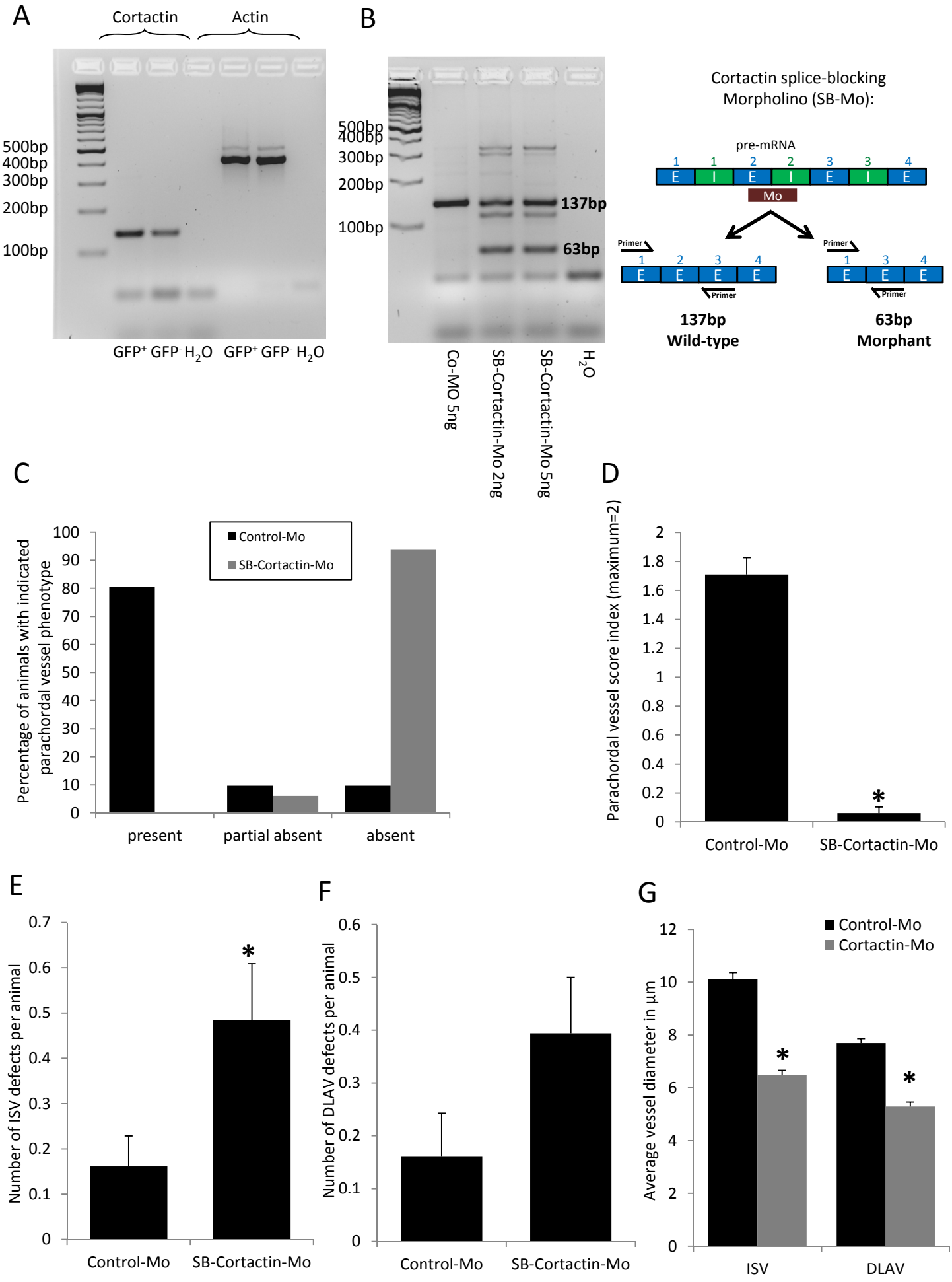

Supplementary Figure 8: Kaluza et al.

EMBOJ-2011-77252R

A

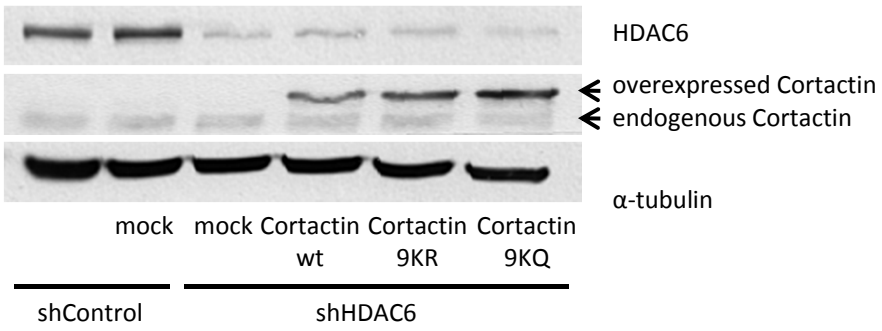

B

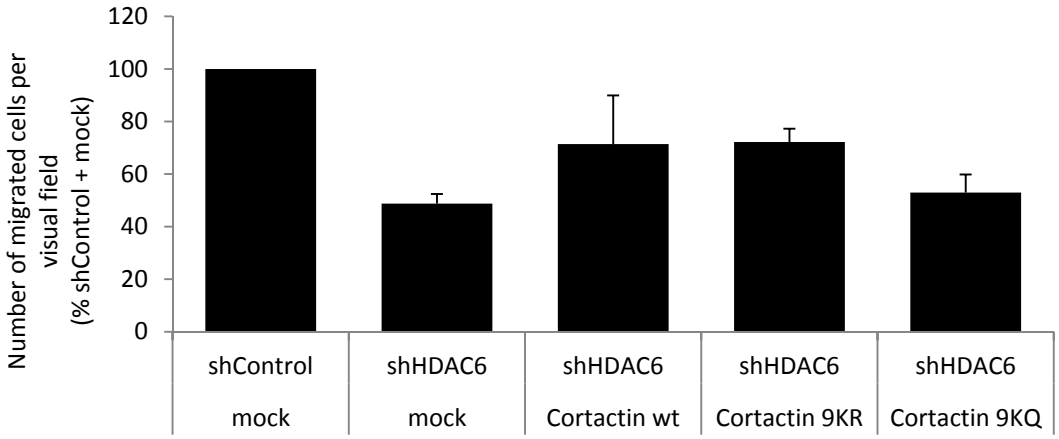

C

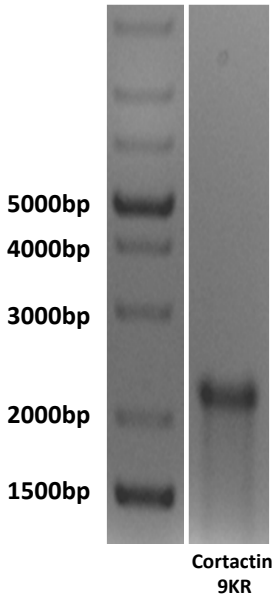

D

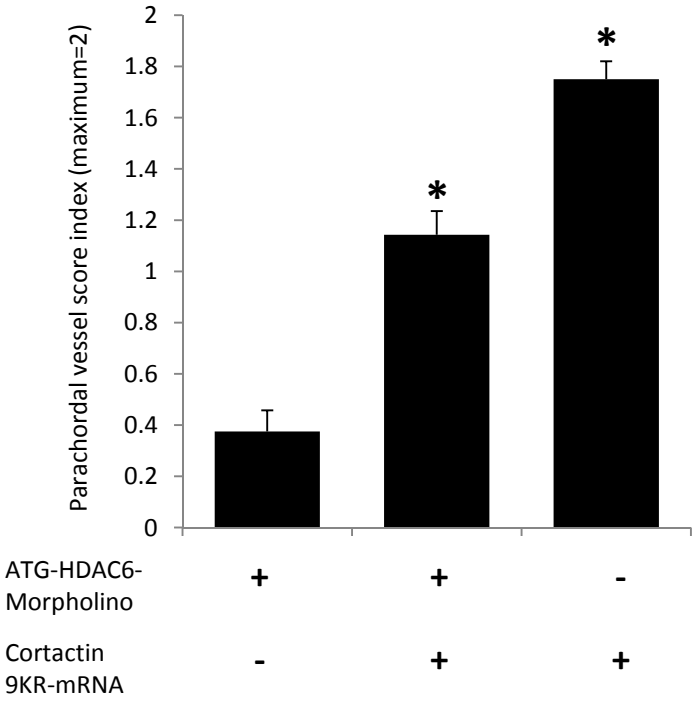

E

Supplementary Figure 9: Kaluza et al.

EMBOJ-2011-77252R